


Role of electronic excitation on the anomalous magnetism of elemental copperSudip Pal¹,* Sumit Sarkar, Kranti Kumar, R. Raghunathan, R. J. Choudhary, A. Banerjee², and S. B. Roy¹
UGC-DAE Consortium for Scientific Research, University Campus, Khandwa Road, Indore 452001, India (Received 28 September 2021; revised 15 December 2021; accepted 2 February 2022; published 16 February 2022)

The magnetic susceptibility of elemental copper (Cu) shows an anomalous rise at low temperatures superimposed on the expected atypical diamagnetic response. Such temperature-dependent susceptibility, which is also known as the Curie tail, cannot be explained on the basis of the Larmor diamagnetic and Pauli paramagnetic contributions expected in Cu. Using valence band resonant photoemission spectroscopy results and density functional theory calculations, we show the magnetic anomaly appears due to the presence of holes in the Cu 3*d* band, which originates from a thermally excited electronic configuration. Our study therefore highlights that the Curie tail, which is generally overlooked presuming it is either due to paramagnetic impurities or defects, can in fact be intrinsic to a material, and even simple systems such as elemental Cu are susceptible to electronic excitations giving rise to an anomalous magnetic state.

DOI: [10.1103/PhysRevB.105.L060406](https://doi.org/10.1103/PhysRevB.105.L060406)

Research on magnetism for the past several decades has been devoted to understanding the transition between a disordered paramagnetic and an ordered magnetic ground state. Interestingly, several materials exhibit an unexpected upturn in the magnetic susceptibility at very low temperatures (typically below 50 K) without any subsequent phase transition to an ordered magnetic state. This anomalous upturn is often termed as the Curie tail and is generally attributed to an extrinsic origin such as the presence of paramagnetic impurities or defects resulting from the synthesis process [1–8]. This anomaly is now becoming more common in a wide range of complex materials. For example, such behavior has recently been found in exotic quantum spin liquids such as Sr₃CuSb₂O₉ and 1*T*-TaS₂ as well as topological materials such as TaSe₃ [9,10]. So, it is important to carefully probe and microscopically understand this anomalous magnetic behavior. This will reveal whether the Curie tail always has an extrinsic origin or in some cases it can be intrinsic to the material.

In compounds, the complex atomic and electronic structures make it difficult to clearly understand the intrinsic mechanisms that govern the overall magnetic properties. In this context, an elemental metal such as copper can be a very suitable starting point. Elemental copper has the electronic configuration Cu : [Ar]3*d*¹⁰4*s*¹, and hence we would expect only two contributions to the overall magnetic susceptibility, namely, the diamagnetism from the completely filled 3*d* orbital and a Pauli paramagnetic contribution of the half-filled 4*s* electrons [11–13]. As both these contributions are temperature independent, the overall magnetic susceptibility of Cu should also be independent of temperature. But, a few decades back, studies on the magnetic behavior of about 99.99% pure elemental copper (Cu) have shown an anomalous temperature dependence of magnetic susceptibility, indicating the presence

of an additional but unusual contribution at low temperatures [14,15]. Here, we show that the magnetic susceptibility of elemental Cu is indeed temperature dependent at low temperatures. However, contrary to the conventional wisdom that the Curie tail is related to the presence of paramagnetic impurities, it originates from the electronic excitations.

We have recorded the temperature (*T*) and magnetic field (*H*) dependent magnetic response of 99.99% pure elemental Cu. Our x-ray fluorescence (XRF) measurement revealed about a 0.01% transition metal impurity which can potentially lead to a paramagnetic tail at low temperature [16]. However, even with such a paramagnetic impurity, the overall magnetic behavior cannot be accounted. Using resonant photoemission spectroscopy, we found the presence of hole in the 3*d* band. This creates an intrinsic spin moment ($s = \frac{1}{2}$) on a fraction of copper atoms giving rise to an additional Curie-like paramagnetic contribution. Importantly, the concentration of holes reduces with a decrease in temperature. Our results thus show that the observed anomalous magnetic behavior of copper is intrinsic in nature.

Magnetic measurements were carried out in a superconducting quantum interference device (SQUID) magnetometer (M/S Quantum Design, USA). The resonating valence band spectra (VBS) were recorded at different photon energies in the range of 60–76 eV using the angle integrated photoemission spectroscopy (AIPES) beamline at the Indus-1 synchrotron source at RRCAT, Indore, India. The XRF measurement has been performed at the XRF beamline on the Indus-2 synchrotron radiation source at RRCAT [16]. The density of states (DOS) has been calculated within the framework of density functional theory (DFT) by employing projector augmented-wave (PAW) potentials using the Vienna *ab initio* simulation package (VASP) [16,17].

The main panel of Fig. 1 shows the temperature dependence of dc susceptibility at $H = 2$ kOe. The susceptibility at 300 K is -1.64×10^{-7} emu/(g Oe), and ensures the dominating diamagnetic nature of the sample. In the isothermal *M*-*H* curve at $T = 300$ K (inset of Fig. 1) *M* is negative

*sudip.pal111@gmail.com

†sbroy@csr.res.in

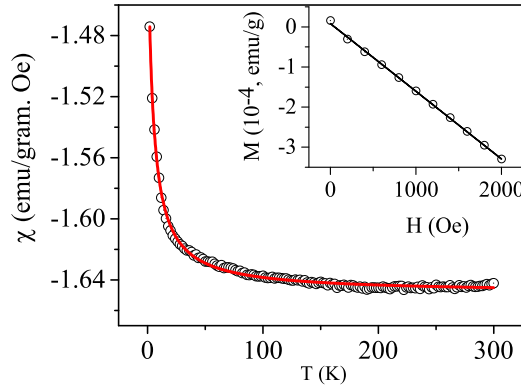


FIG. 1. χ - T curve measured at $H = 2$ kOe. The inset shows the M - H curve at $T = 300$ K. The red line in the main panel shows the fitted curve using $\chi = \chi_0 + \frac{C}{T-T_0}$.

and varies linearly with H . The susceptibility ($\chi = M/H$) at 300 K, obtained from the slope of the M - H curve is $\chi = -1.66 \times 10^{-7}$ emu/(g Oe). A diamagnetic sample should show a negative and temperature-independent susceptibility. However, our experimental results indicate that M is nearly constant down to 150 K, but at further lower temperatures, M starts to increase. This rise in M below 150 K appears similar to Curie-Weiss paramagnetic-like behavior which is known as the Curie tail. For an elemental metal such as copper with completely filled $3d$ and half-filled $4s$ shells, we expect diamagnetic and Pauli paramagnetic contributions. As both these contributions should be temperature independent, the low-temperature Curie tail is rather surprising. Such a temperature dependence of magnetization is qualitatively similar to those reported earlier [14,15]. Note that the susceptibility can be fitted considering an additional Curie-Weiss-like term ($\frac{C}{T-T_0}$) as shown in Fig. 1 (red line), where C is a constant giving us the value of the impurity spin. However, we will show in the following sections that such a fitting would be meaningless, because C is actually temperature dependent due to the intrinsic property of copper.

In order to understand this anomalous magnetic behavior, we analytically calculate the diamagnetic and Pauli paramagnetic contributions to the total magnetic susceptibility. In the case of elemental Cu with an atomic number $Z = 29$, the conventional electronic configuration is $[\text{Ar}]3d^{10}4s^1$. The Larmor diamagnetic contribution can be estimated from [11,12]

$$\chi_D = -0.79Z_i \times 10^{-6} \langle (r/a_0) \rangle^2 \text{ emu/(g Oe)}. \quad (1)$$

Here, Z_i is the number of electrons in the atom, r is the atomic radius (for Cu, $r = 1.28 \text{ \AA}$) and a_0 is the Bohr radius. Taking $\langle (r/a_0) \rangle = 2.42$, the diamagnetic susceptibility can be estimated as $\chi_D = -20.30 \times 10^{-7}$ emu/(g Oe). In addition, conduction electrons give rise to a positive magnetic susceptibility, known as the Pauli paramagnetism [11,13]. At $T = 0$ K, the Pauli paramagnetic susceptibility is written as

$$\chi_P = \mu_B^2 g(E_F), \quad (2)$$

where $g(E_F)$ is the total density of states at the Fermi level, which can be calculated using DFT. In case of Cu, it is obtained to be 0.10 eV^{-1} (see Fig. 3 inset). Substituting this

in Eq. (2) gives the Pauli paramagnetic susceptibility $\chi_P = 0.51 \times 10^{-7}$ emu/(g Oe). It may be noted that at finite temperature, smearing of the Fermi surface introduces a very small correction to Eq. (2). However, in the case of Cu, due to a very large Fermi temperature (around 80 000 K), this correction is negligible up to room temperature. Now, the net susceptibility can be obtained by summing the diamagnetic and paramagnetic contributions ($\chi = \chi_D + \chi_P$) which gives $\chi = -19.79 \times 10^{-7}$ emu/(g Oe). Our calculated total susceptibility is one order of magnitude larger than the experimental data, suggesting the presence of additional contributions apart from χ_D and χ_P , and this warrants an explanation.

The results of our XRF measurements suggested the presence of about 0.01% of Mn impurity in the present Cu sample [16]. Therefore, it would be instructive to understand the effect of electron delocalization on the effective moment of a Mn atom with an electron configuration $[\text{Ar}]3d^54s^2$ in a copper lattice. So, we performed DFT calculations on a $5 \times 5 \times 5$ supercell of copper containing 500 atoms. For the pure copper case, our calculations show that the copper atoms have a negligible magnetic moment of $0.02\mu_B$. We also carried out DFT calculations of this supercell by replacing a copper atom with a manganese atom. This corresponds to an effective impurity concentration of 0.2%. It should be noted that our goal here is not to mimic the experimental impurity concentration, but rather to identify the role of electron delocalization on the magnetic moment of copper and manganese atoms. Our calculations show that the presence of manganese also enhances the moment of copper atoms to $0.06\mu_B$, but still the copper moment is negligible. The magnetic moment of manganese is equivalent to spin, $S_{\text{Mn}} = 0.009$, much lesser compared to the expected $S = \frac{5}{2}$ for five unpaired electrons.

Now that we know the magnetic moments of manganese, we can add the paramagnetic contribution using the Curie-Weiss relation with the diamagnetic and Pauli paramagnetic contributions to obtain the total magnetic susceptibility $\chi = \chi_D + \chi_{\text{Pauli}} + \chi_{\text{PM}}^{\text{Mn}}(T)$:

$$\begin{aligned} \chi_{\text{PM}}^{\text{Mn}}(T) &= \frac{N_A g^2 \mu_B^2 S_{\text{Mn}}(S_{\text{Mn}} + 1)}{3k_B T} \\ &= \frac{0.0826 \times 10^{-7}}{T} \text{ emu/g Oe}. \end{aligned} \quad (3)$$

Here, S_{Mn} corresponds to the Mn spin moment, N_A is the Avogadro number, μ_B is the Bohr magneton, g is the gyromagnetic ratio which is taken to be 2, k_B is the Boltzmann constant, and T is the temperature. The calculated susceptibility is plotted as a function of temperature in Fig. 2(a), together with the experimental data. Note that the addition of 0.01% Mn impurity cannot reproduce the experimentally observed susceptibility behavior, which suggests the presence of an additional contribution which is perhaps intrinsic to copper.

Generally in $3d$ transition metals, the $3d$ and $4s$ orbital energies are close enough. This allows for electrons to exist in two possible electronic states. Our conventional wisdom suggests that copper exists in the $[\text{Ar}]3d^{10}4s^1$ configuration, whereas an energetically $[\text{Ar}]3d^94s^2$ electronic state is also possible. At absolute zero, the Fermi-Dirac function is a step function where all the states below the Fermi level are filled and all those states above E_F are empty. This corresponds to

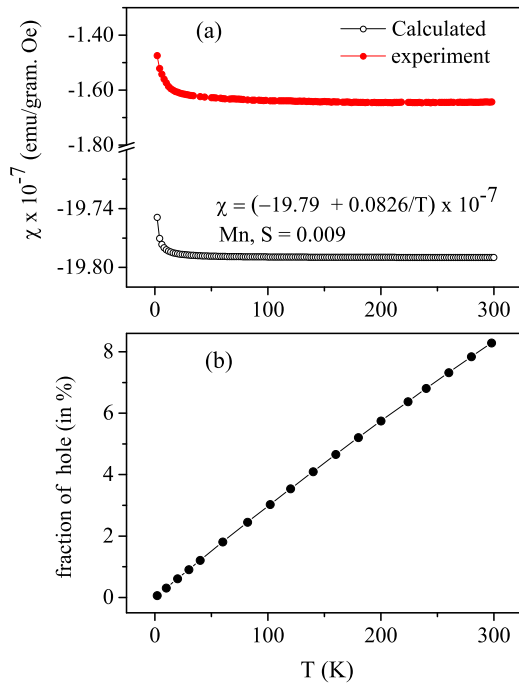


FIG. 2. (a) Experimental and calculated χ - T data. The calculated temperature variation of χ has been obtained by considering the diamagnetic and Pauli paramagnetic contribution of Cu and a Curie-Weiss paramagnetic contribution of 0.01% of Mn present in the sample. (b) Fraction of the hole estimated by using Eq. (5) from the additional susceptibility observed in experiment, as compared to the calculated value.

the electron configuration $[\text{Ar}]3d^{10}4s^1$. At temperatures above absolute zero, due to thermal energy some of the electrons can get excited from the $3d$ to $4s$ band. This hypothesis is further supported by our partial DOS calculated using DFT which is presented in Fig. 3. We notice that the DOS weights for the $3d$ band are nonzero even above the Fermi level. These observations suggest that the $3d$ band of copper potentially has holes. This can open up the possibility of unpaired electrons in the $3d$ band leading to intrinsic magnetic moments

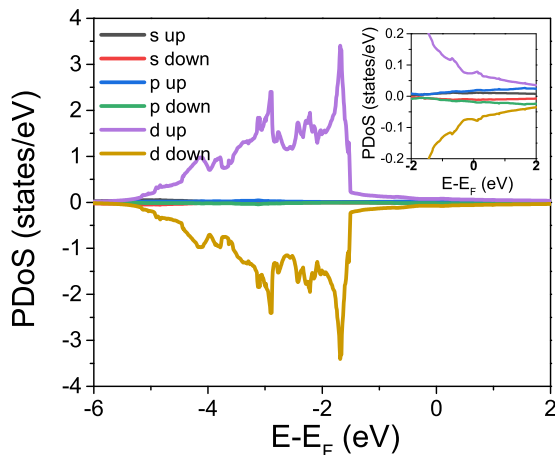


FIG. 3. Partial density of states near E_F at $T = 0$ obtained from DFT. At E_F , the total DOS is 0.1 eV^{-1} .

on a fraction of copper sites due to the instability created by a fluctuation between $[\text{Ar}]3d^{10}4s^1 \Leftrightarrow [\text{Ar}]3d^94s^2$ electronic states, due to the thermal energy. The $3d^{10}4s^1$ configuration of copper gives a diamagnetic plus Pauli paramagnetic configuration, whereas a $3d^94s^2$ configuration would result in an additional Curie-Weiss-like paramagnetic contribution. Therefore, the magnetic property of copper is governed by the competition between these two sets of contributions,

$$\chi_D + \chi_{\text{PPM}} \Leftrightarrow \chi_{\text{PM}} + \chi_D + \chi_{\text{PPM}}, \quad (4)$$

where the left- and right-hand sides correspond to $3d^{10}4s^1$ and $3d^94s^2$ configurations, respectively. In the light of holes in the $3d$ band, we now discuss the observed temperature dependence of magnetic susceptibility in two temperature regimes: (i) $T > 150 \text{ K}$ and (ii) $T < 150 \text{ K}$. In region (i), say 300 K , there will be significant number of holes in the $3d$ band leading to a larger concentration of paramagnetic ions. The smearing of electrons around the Fermi level decreases as the temperature is lowered. Consequently, the concentration of paramagnetic copper atoms due to the intrinsic moment of copper also decreases. As the paramagnetic susceptibility is inversely related to the temperature, the overall susceptibility remains more or less constant in this temperature range. The temperature dependence of susceptibility in regime (ii) shows a Curie tail. In this temperature regime, the paramagnetic contributions both from the Mn impurity and the intrinsic moment of copper become dominant as the temperature is lowered. At the same time, as the Fermi smearing reduces with a decrease in temperature, the concentration of the intrinsic moment also decreases. However, the final behavior will depend upon the rate at which the concentration of the intrinsic moment decreases with temperature. Typically at temperatures close enough to absolute zero, the electron configuration of copper would tend to $[\text{Ar}]3d^{10}4s^1$ and the Curie tail would be governed solely by the Mn impurity. With this argument, the total susceptibility of copper can be written as follows.

$$\chi(T) = \chi_D + [1 + x(T)]\chi_{\text{PPM}} + \chi_{\text{PM}}^{\text{Mn}}(T) + x(T)\chi_{\text{PM}}^{\text{Cu}}(T). \quad (5)$$

The terms in the above equation correspond to contributions from diamagnetism, Pauli paramagnetism, paramagnetism due to Mn moments, and paramagnetism due to Cu moments, respectively. The factor $x(T)$ is the concentration of Cu moments at temperature T due to the Fermi smearing, and it can be calculated considering that the mismatch between the experimental and calculated susceptibility is due to the temperature variation of x , which is shown in Fig. 2(b). The concentration of Cu moments x reduces with a decrease in temperature.

To further validate our hypothesis of intrinsic copper moments due to the presence of holes in the $3d$ band, we recorded the valance band spectrum (VBS) in the vicinity of the Fermi level. Figure 4(a) shows the data recorded at $T = 300 \text{ K}$ at an incident photon energy of 68 eV . The overall response has been fitted by Gaussian peak shapes, and referred to as A, B, C, and D as shown in Fig. 4(a). The background is corrected by using the Shirley method. Further, we have performed resonating photoemission spectroscopy in the incident photon energy range of $60\text{--}76 \text{ eV}$, which covers the $\text{Cu } 3p \rightarrow 3d$

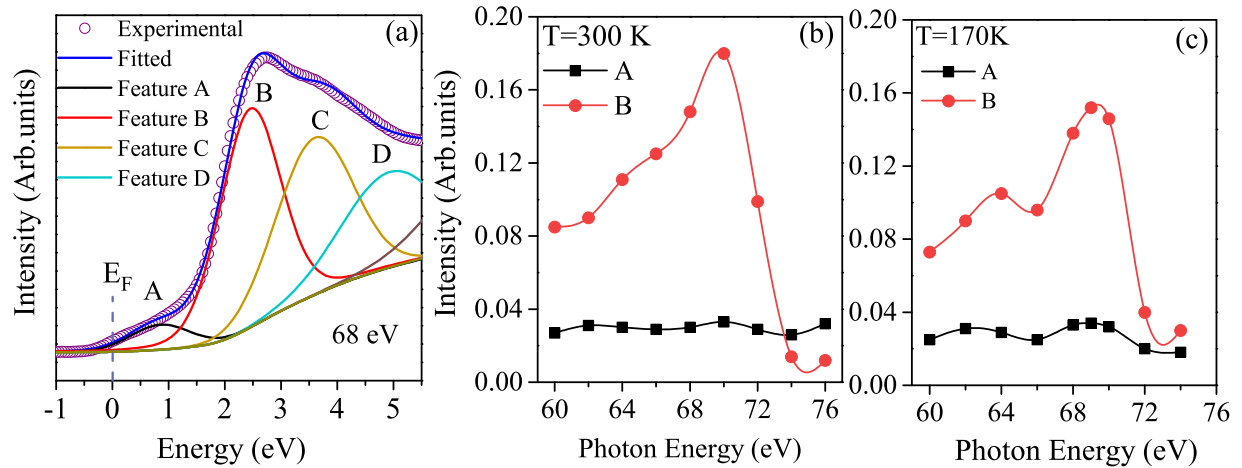
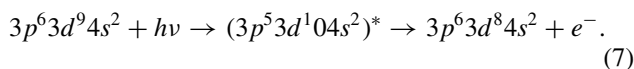
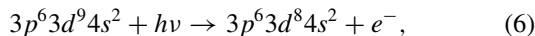


FIG. 4. (a) Experimental data of RPES at $T = 300$ K at an incident photon energy of 68 eV fitted by considering Gaussian shape peaks and Shirley background, (b) and (c) show the CIS plot of the near E_F spectral features at $T = 300$ and 170 K, respectively, obtained from the fitting of the valance band measured at each incident photon energy.

excitation energy and shows a maximum at $E = 70$ eV. All the data recorded at different incident energies have been fitted similar to Fig. 4(a). Features A and B centered around 0.8 and 2.5 eV are mainly our region of interest, because it is dominated by the Cu 4s and 3d hybridized band, as observed in our DFT calculated density of states (DOS), as well as previous literature [18]. We have determined the spectral intensity of these features from the integrated area of these features after a background correction and plotted them as a function of incident photon energy in Figs. 4(b) and 4(c). This is known as constant initial state (CIS) plot. The CIS of feature A at 0.8 eV does not show any significant variation with the incident photon energy and is probably dominated by the 4s orbital as the photoionization cross section of Cu 4s is much less than the 3d orbital [19]. The feature at B at 2.5 eV monotonically enhances with the increase in incident energy and shows strong resonance at around 70 eV. Here, the resonance occurs due to the quantum-mechanical interference between direct photoemission from 3d and intra-atomic excitation of $3p \rightarrow 3d$, followed by super Coster-Kronig decay which is shown below:



The resonance enhancement near Cu, $3p \rightarrow 3d$ excitation energy, indicates the presence of a 3d hole, i.e., $3d^9 4s^2$ valence state of Cu. The population of this state should reduce with the decrease in temperature due to reduced thermal energy. Therefore, the relative resonance intensity of the feature should

be suppressed with the lowering of temperature. To confirm this, we have carried out resonant photoelectron spectroscopy (RPES) measurements at $T = 170$ K, also shown in Fig. 4(c). We observe that the width and the intensity of the resonance near 70 eV in feature B is reduced at $T = 170$ K relative to 300 K [16]. It indicates that the bandwidth corresponding to the $3d$ - $4s$ overlapping has reduced at lower temperature, which is a manifestation of the reduced $3d^9 4s^2$ configuration. Therefore it confirms our earlier hypothesis. It may be noted that the RPES study in this energy range is highly surface sensitive [20]. Moreover, the positive value of the Seebeck coefficient may be an indication of the presence of holes in elemental Cu, however it is still under debate [21–24].

The temperature and magnetic field dependences of the dc susceptibility of elemental Cu show dominant diamagnetism and an additional Curie-Weiss-like behavior at low temperatures. The calculated dc susceptibility based on the textbook formula for orbital diamagnetism and Pauli paramagnetism is insufficient to explain the magnetic behavior in the measured range of temperature. DFT results indicate the presence of small but significant contributions from the 4s orbital of Cu. Based on these results, we propose a mechanism involving a fluctuation between two electronic states of copper. This leads to competition between different magnetic contributions due to the presence of holes in the 3d band, which is further confirmed by RPES experiments. We conclude that the anomalous Curie-Weiss-like paramagnetic behavior arises due to the presence of holes in a certain fraction of Cu atoms, which is excited by thermal energy.

S.P. acknowledges Dr. L. S. Sarath Chandra and Md. Akhlaq for help in analyzing the XRF data.

- [1] S. Lebernegg, A. A. Tsirlin, O. Janson, and H. Rosner, *Phys. Rev. B* **88**, 224406 (2013).
 [2] Y. Tang, C. Peng, W. Guo, J.-F. Wang, G. Su, and Z. He, *J. Am. Chem. Soc.* **139**, 14057 (2017).

- [3] M. Cui, Z. He, N. Wang, Y. Tang, W. Guo, S. Zhang, L. Wang, and H. Xiang, *Dalton Trans.* **45**, 5234 (2016).
 [4] S. Das, X. Zong, A. Niazi, A. Ellern, J. Q. Yan, and D. C. Johnston, *Phys. Rev. B* **76**, 054418 (2007).

- [5] C.-K. Hsu, D. Hsu, C.-M. Wu, C.-Y. Li, C.-H. Hung, C.-H. Lee, and W.-H. Li, *J. Appl. Phys.* **109**, 07B528 (2011).
- [6] R. Schmidt, J. Wu, C. Leighton, and I. Terry, *Phys. Rev. B* **79**, 125105 (2009).
- [7] J. Q. Yan, J. S. Zhou, and J. B. Goodenough, *Phys. Rev. B* **70**, 014402 (2004).
- [8] D. Phelan, D. Louca, S. Rosenkranz, S.-H. Lee, Y. Qiu, P. J. Chupas, R. Osborn, H. Zheng, J. F. Mitchell, J. R. D. Copley, J. L. Sarrao, and Y. Moritomo, *Phys. Rev. Lett.* **96**, 027201 (2006).
- [9] S. Kundu, A. Shahee, A. Chakraborty, K. M. Ranjith, B. Koo, J. Sichelschmidt, M. T. F. Telling, P. K. Biswas, M. Baenitz, I. Dasgupta, S. Pujari, and A. V. Mahajan, *Phys. Rev. Lett.* **125**, 267202 (2020).
- [10] A. Ikhwan Us Saleheen, R. Chapai, L. Xing, R. Nepal, D. Gong, X. Gui, W. Xie, D. P. Young, E. W. Plummer, and R. Jin, *npj Quantum Mater.* **5**, 53 (2020).
- [11] N. W. Ashcroft and N. D. Mermin, *Solid State Physics* (Cengage Learning, Boston, 1975).
- [12] J. M. D. Coey, *Magnetism and Magnetic Materials* (Cambridge University Press, Cambridge, UK, 2010).
- [13] S. Blundell, *Magnetism in Condensed Matter* (Oxford University Press, Oxford, UK, 2001).
- [14] R. Bowers, *Phys. Rev.* **102**, 1486 (1965).
- [15] F. Bitter, A. R. Kaufmann, C. Starr, and S. T. Pan, *Phys. Rev.* **60**, 134 (1941).
- [16] See Supplemental Material at <http://link.aps.org/supplemental/10.1103/PhysRevB.105.L060406> for the analysis of the XRF data, details about our DFT calculations, short description about RPES, and temperature dependence of magnetization of the sample holder used for magnetic measurements.
- [17] G. Kresse and J. Furthmüller, *Phys. Rev. B* **54**, 11169 (1996); G. Kresse and D. Joubert, *ibid.* **59**, 1758 (1999).
- [18] A. Jedidi, S. Rasul, D. Masih, L. Cavallo, and K. Takanebe, *J. Mater. Chem. A* **3**, 19085 (2015).
- [19] J. J. Yeh and I. Lindau, *At. Data Nucl. Data Tables* **32**, 1 (1985).
- [20] S. Hufner, *Photoelectron Spectroscopy: Principles and Applications*, 3rd ed. (Springer, Berlin, 1995).
- [21] H. Jones, *Proc. Phys. Soc. London, Sect. A* **68**, 1191 (1955).
- [22] S. Fujita, H. C. Ho, and Y. Okamura, *Int. J. Mod. Phys. B* **14**, 2231 (2000).
- [23] S. Fujita and A. Suzuki, Quantum theory of thermoelectric power (Seebeck coefficient), in *Electromotive Force and Measurement in Several Systems*, edited by S. Kara (InTechOpen, Rijeka, Croatia, 2011).
- [24] B. Xu and M. J. Verstraete, *Phys. Rev. Lett.* **112**, 196603 (2014).